# True Direction Equilibrium Flux Method applications on rectangular 2D meshes

M. N. Macrossan*, M. R. Smith*, M. V. Metchnik† and P. A. Pinto†

*Centre for Hypersonics, The University of Queensland, Brisbane, 4072, Australia
†Steward Observatory, University of Arizona, 933 N Cherry Av, Tucson, AZ 85722-0065, USA

**Abstract.** In conventional 2D or 3D continuum solvers, the fluxes are 'direction decoupled'; 1D flux calculations are performed in the direction normal to the cell interfaces, and fluxes are exchanged only between cells which share a cell interface. On a 2D structured grid, for example, the fluxes flow in two coordinate directions and never flow in one time step between cells which are diagonally contiguous but do not have a common interface. Cook [1] shows that direction decoupled methods may produce unphysical results such as negative temperatures or densities where strong shocks occur or interact. Pullin [2] proposed the Equilibrium Flux Method (EFM) in which the molecular fluxes in a 1D flow were computed analytically, assuming a Boltzmann distribution in each cell. EFM has been used in 2D [3] flows by using conventional direction decoupling. Here, EFM is extended to 2D without direction decoupling; fluxes flow between any two cells in a Cartesian grid. This 'True Direction Equilibrium Flux Method' or (TDEFM) is the analytical form of the infinite collision limit of DSMC but has none of the statistical scatter associated with the particle nature of DSMC. We calculate an unsteady 2D implosion on a regular Cartesian grid, where the flow structures are not aligned with the grid. A circular region of low-pressure gas (centered at the origin) is surrounded by the same gas at a higher pressure with an initial circular discontinuity between the two regions. A circular shock propagates towards the origin, where it is reflected. An expansion wave travels outwards. All methods used here were first order accurate in space. TDEFM results are compared with direction decoupled results using the 1D fluxes of an approximate Riemann solver, and the 1D EFM fluxes. TDEFM captures the circular symmetry while the direction decoupled methods introduce unphysical asymmetries. The results show that on a uniform rectangular mesh TDEFM can capture flows which are not aligned with the grid with greater accuracy than direction decoupled methods. TDEFM requires 1% less CPU time than the direction decoupled Riemann solver

**Keywords:** Kinetic Theory of Gasses, CFD, DSMC, EPSM, EFM, TDEFM, Direct Simulation, Euler Equations
**PACS:** 31.15.Qg, 34.10.+x,47.10.A-,47.11.-j,47.11.Mn,47.45.Ab,47.45.-n

## INTRODUCTION

In a finite volume CFD method for unsteady flow fluxes of mass, momentum and energy are exchanged between cells over a series of small time steps. The conventional approach, which we will refer to as *direction decoupling*, is to estimate fluxes across interfaces in a regular array of cells by using a one-dimensional flux expression based on the component of flow velocity normal to the interface. Fluxes are not exchanged between diagonally adjacent cells since they share no cell interface, whereas the local flow conditions might indicate that the fluxes should flow diagonally. The direction decoupling imposed by the numerical method requires that the fluxes reach a diagonally adjacent cell in two time-steps.

Bird's Direct Simulation Monte-Carlo method simulates a rarefied flow by following the motion and collisions of a large number of simulator particles as they move through the flow. DSMC in the high collision rate limit has been used as an Euler solver [2, 4, 5] and as the 'continuum' part of a hybrid DSMC/continuum solver. DSMC is generally more robust than a conventional Euler solver but suffers from statistical scatter which requires large amounts of CPU power to reduce to acceptable limits. One reason for DSMC's stability is that the fluxes of mass, momentum and energy are carried by particles which move in the physically correct directions; in any time step fluxes may flow from any cell to any other cell in the computational domain. In other words DSMC is not a direction decoupled method. Cook [1] shows that when the cell structure is not well aligned with the physical structures in the flow, direction decoupled methods may produce unphysical results such as negative temperatures or densities where strong shocks occur or interact. These solvers may also produce asymmetrical results where symmetrical results are theoretically expected or required.

Macrossan *et al.* [6] used the 'Particle Flux Method' to mimic the effect of high-collision rate limit DSMC. Some statistical scatter was unavoidable, since particles, which were generated statistically within each cell, were used to carry the fluxes to other cells. Pullin [2] proposed the Equilibrium Flux Method (EFM) in which the fluxes carried

by particles having velocities conforming to the local Maxwell-Boltzmann distribution were calculated analytically for the limit of an infinite number of particles. EFM eliminates the statistical scatter associated with the effectively equivalent particle flux methods. When EFM was used in 2D and 3D flows [7, 3, 9, 10] the conventional direction decoupling approach described above was used.

Since the EFM fluxes are just the amounts of mass, momentum and energy transported by molecules in free-molecular flight there is no need, other than for simplicity, to use direction decoupling when EFM is applied in two or three dimensions. Here we derive the expressions for the fluxes carried by molecules, originating in a rectangular cell with velocities selected from the Maxwell-Boltzmann distribution, and moving in a specified time of flight to *any* other rectangular region. Mass, energy and momentum are all perfectly conserved. Since this is an updated version of Pullin's EFM [2] we call this method the *True Direction Equilibrium Flux Method* (TDEFM). The time step is in effect a mean collision time, and hence an inherent dissipation arises in TDEFM which is proportional to the time step. In the test case considered we restrict the time step so that molecular fluxes flow to nearest neighbor cells only. In that case simplified (limiting) fluxes expressions can be used. These limiting flux expressions are given by Smith *et al.* [12]. The TDEFM flux calculations used here are restricted to 1st order accuracy in space (no gradients of flow properties within cells). Results of this true direction flux method are compared with those obtained with direction coupling when the 1D fluxes are obtained by two different methods: the kinetic EFM flux expressions and an approximate Riemann solver [11].

## TDEFM

Derived below are the expressions for the mass, momentum and energy carried by molecules in free-molecular flight for time $t$, starting from a rectangular region (in 2D) to any other rectangular region. Internal energy, *i.e.* energy stored in the molecular structure, is included in the energy flux expressions so monoatomic, diatomic or polyatomic gases can be simulated.

Uniform conditions are assumed within the cell from which the molecules originate (*i.e.* there are no gradients of density, mean velocity or temperature within the cell) and all the molecules within the cell have velocities conforming to the same Maxwell-Boltzmann distribution. The distribution function for components of molecular velocity, $v_j \equiv v_x$ or $v_y$ or $v_z$, has the Maxwell-Boltzmann form

$$f(v_x, v_y, v_z) = g(v_x)\, g(v_y)\, g(v_z)$$

where

$$g(v_j) = \frac{1}{\pi^{1/2} c_m} \exp\left(-\frac{(v_j - V_j)^2}{c_m^2}\right),\ V_j \equiv \bar{v}_j = \int_{-\infty}^{\infty} v_j g dv_j \text{ and } c_m = (2RT)^{-1/2}.$$

In other words, the fraction of molecules having a velocity $v_x$ in the range $v_x \rightarrow v_x + dv_x$ is $g(v_x)\, dv_x$ and similar expressions hold for $v_y$ and $v_z$. The components of the mean flow velocity (mean molecular velocity) in any cell are $V_x$ and $V_y$ (and $V_z = 0$ for 2D flow), the mass density is $\rho = m_p n$, where $m_p$ is the mass of one molecule and $n$ is the number density (molecules/m$^3$). The random thermal velocity is $c_j = v_j - V_j$ and the three components of translational kinetic temperature are given by $RT_j = \int_{-\infty}^{\infty} c_j^2 g\, dv_j$ where $R$ is the ordinary gas constant. All kinetic temperatures are the same and the 'overall' kinetic temperature is $T = (T_x + T_y + T_z)/3 = T_x = T_y = T_z$. Setting $s \equiv \sqrt{RT}$ and $m \equiv V_j$ the expression for $g(v)$ can be rewritten as:

$$g(v_j) = \frac{1}{\sqrt{2\pi} s} \exp\left(\frac{-(v_j - m)^2}{2s^2}\right) \tag{1}$$

The probability of a particle with a velocity between $a$ and $b$, or $P_m$, is:

$$P_m = \int_a^b \frac{1}{\sqrt{2\pi} s} \exp\left(\frac{-(v_j - m)^2}{2s^2}\right) dv_j \tag{2}$$

Referring to Fig. 1, for a particle at location $x$ to travel to a location between $x_l$ and $x_r$ in a time space $t$, the velocity range falls between $(x - x_l)/t$ and $(x - x_r)/t$. Therefore, we can reevaluate the integral in Eq. 2 to obtain:

$$P_m = \int_{(x-x_l)/t}^{(x-x_r)/t} \frac{1}{\sqrt{2\pi} s} \exp \frac{-(v_x - m)^2}{2s^2}\, dv_x = \frac{1}{2}\left[\text{erf}\left(\frac{mt + x - x_l}{\sqrt{2} st}\right) - \text{erf}\left(\frac{mt + x - x_r}{\sqrt{2} st}\right)\right] \tag{3}$$

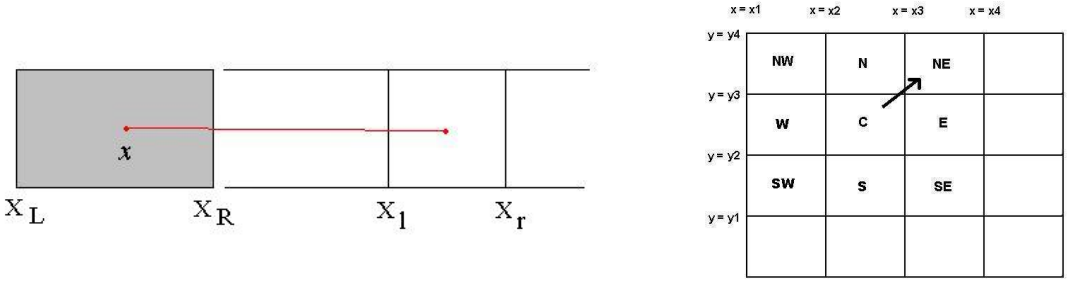


**FIGURE 1.** (Left) Particle moving from x (between $x_L$ and $x_R$) to a region between $x_l$ and $x_r$. For the derivations used here, $x_r \geq x_l$ & $x_R \geq x_L$. (Right) Structured, uniform rectangular mesh used in TDEFM example. Molecules start from a random position within cell $C$, with a velocity selected from the Maxwell-Boltzmann distribution,and flow (in a small time $t$) to any of the eight contiguous cells labelled NE, N, NW, W, SW, S, SE and E.

We will call $f_{ME}$ the fraction of particles from the region between $x_L$ and $x_R$ having the specified velocities. This is:

$$f_{ME} = \int_{x_L}^{x_R} \frac{1}{2}\left[\text{erf}\left(\frac{mt+x-x_l}{\sqrt{2}st}\right) - \text{erf}\left(\frac{mt+x-x_r}{\sqrt{2}st}\right)\right] dx \tag{4}$$

The general expression for fraction of mass flow to any region $x_l - x_r$ from $x_L - x_R$ is:

$$\begin{aligned} f_{ME} \quad &= \tfrac{st}{\sqrt{2\pi}}\left[\exp\left(\tfrac{-(mt+x_R-x_l)^2}{2s^2t^2}\right) - \exp\left(\tfrac{-(mt+x_L-x_l)^2}{2s^2t^2}\right) - \exp\left(\tfrac{-(mt+x_R-x_r)^2}{2s^2t^2}\right) - \exp\left(\tfrac{-(mt+x_L-x_r)^2}{2s^2t^2}\right)\right] \\ &-\tfrac{1}{2}(mt+x_R-x_l)\,\text{erf}\left(\tfrac{mt+x_R-x_l}{\sqrt{2}st}\right) - \tfrac{1}{2}(mt+x_L-x_l)\,\text{erf}\left(\tfrac{mt+x_L-x_l}{\sqrt{2}st}\right) \\ &-\tfrac{1}{2}(mt+x_R-x_r)\,\text{erf}\left(\tfrac{mt+x_R-x_r}{\sqrt{2}st}\right) + \tfrac{1}{2}(mt+x_L-x_r)\,\text{erf}\left(\tfrac{mt+x_L-x_r}{\sqrt{2}st}\right) \end{aligned} \tag{5}$$

Putting $x_l = x_R$ in Eq. 5 gives the fraction of mass flowing into the immediately adjacent cell:

$$\begin{aligned} \textstyle\int_{x_L}^{x_R} P_m\,dx \quad &= \tfrac{st}{\sqrt{2\pi}}\left[\exp\left(\tfrac{-m^2}{2s^2}\right) - \exp\left(\tfrac{-(mt+x_L-x_R)^2}{2s^2t^2}\right) - \exp\left(\tfrac{-(mt+x_R-x_r)^2}{2s^2t^2}\right) - \exp\left(\tfrac{-(mt+x_L-x_r)^2}{2s^2t^2}\right)\right] \\ &+\tfrac{1}{2}(mt)\,\text{erf}\left(\tfrac{m}{\sqrt{2}s}\right) - \tfrac{1}{2}(mt+x_L-x_R)\,\text{erf}\left(\tfrac{mt+x_L-x_R}{\sqrt{2}st}\right) \\ &-\tfrac{1}{2}(mt+x_R-x_r)\,\text{erf}\left(\tfrac{mt+x_R-x_r}{\sqrt{2}st}\right) + \tfrac{1}{2}(mt+x_L-x_r)\,\text{erf}\left(\tfrac{mt+x_L-x_r}{\sqrt{2}st}\right) \end{aligned} \tag{6}$$

The mean velocity of particles (mean momentum per unit mass) from location $x$ finishing between $x_l$ and $x_r$ is:

$$P_p = \int_{(x_l-x)/t}^{(x_r-x)/t} v_x \frac{1}{\sqrt{2\pi}s}\exp\left(\frac{-(v_x-m)^2}{2s^2}\right) dv_x \tag{7}$$

The average velocity of particles moving into region $x_l \leftrightarrow x_r$ from region $x_L \leftrightarrow x_R$ is $f_{PE} = \int_{x_L}^{x_R} P_p dx$. Solving and evaluating this integral from $x_L$ to $x_R$ gives:

$$\begin{aligned} f_{PE} \quad &= \tfrac{mst}{\sqrt{2\pi}}\left[\exp\left(\tfrac{-(mt+x_R-x_l)^2}{2s^2t^2}\right) - \exp\left(\tfrac{-(mt+x_L-x_l)^2}{2s^2t^2}\right) - \exp\left(\tfrac{-(mt+x_R-x_r)^2}{2s^2t^2}\right) - \exp\left(\tfrac{-(mt+x_L-x_r)^2}{2s^2t^2}\right)\right] \\ &-\tfrac{1}{2}\left(m(mt+x_R-x_l)+s^2t\right)\text{erf}\left(\tfrac{mt+x_R-x_l}{\sqrt{2}st}\right) - \tfrac{1}{2}\left(m(mt+x_L-x_l)+s^2t\right)\text{erf}\left(\tfrac{mt+x_L-x_l}{\sqrt{2}st}\right) \\ &-\tfrac{1}{2}\left(m(mt+x_R-x_r)+s^2t\right)\text{erf}\left(\tfrac{mt+x_R-x_r}{\sqrt{2}st}\right) + \tfrac{1}{2}\left(m(mt+x_L-x_r)+s^2t\right)\text{erf}\left(\tfrac{mt+x_L-x_r}{\sqrt{2}st}\right) \end{aligned} \tag{8}$$

The mean energy of particles (per unit mass) moving from $x$ into the region between $x_l$ and $x_r$,$P_e$, is:

$$P_e = \int_{(x_l-x)/t}^{(x_r-x)/t} \frac{(0.5v_x^2+C)}{\sqrt{2\pi}s}\exp\left(\frac{-(v_x-m)^2}{2s^2}\right) dv_x \tag{9}$$

where $C$ is the specific internal energy (J/kg) of a molecule stored in vibrational and rotational degrees of freedom. Each fully excited internal degree of freedom stores $kT/2$ joules of energy per particle, or $RT/2$ joules of energy per kg.

Therefore, $C = \zeta RT/2$, where $\zeta$ is the number of internal degrees of freedom, and is given by $\zeta = (5-3\gamma)/(\gamma-1)$, where $\gamma$ is the ratio of specific heats. Evaluation of the integral in Eq. 9 gives:

$$\begin{aligned} P_e &= \tfrac{1}{4}\left(m^2+s^2+2C\right)\left[\operatorname{erf}\left(\tfrac{mt+x-x_l}{\sqrt{2}st}\right)-\operatorname{erf}\left(\tfrac{mt+x-x_r}{\sqrt{2}st}\right)\right] \\ &+\tfrac{s}{2t\sqrt{2\pi}}\left[(mt+x_l-x)\exp\left(\tfrac{-(mt+x-x_l)^2}{2s^2t^2}\right)-(mt+x_r-x)\exp\left(\tfrac{-(mt+x-x_r)^2}{2s^2t^2}\right)\right] \end{aligned} \tag{10}$$

The fraction of energy in the region $x_L$ to $x_R$ which flows into the region $x_l$ to $x_r$ is

$$\begin{aligned} f_{EE} &= \textstyle\int_{x_L}^{x_R} P_e\,dx = \frac{st\left(m^2+2s^2+2C\right)}{2\sqrt{2\pi}} \\ &\times\left[\exp\left(\tfrac{-(mt+x_R-x_l)^2}{2s^2t^2}\right)-\exp\left(\tfrac{-(mt+x_L-x_l)^2}{2s^2t^2}\right)-\exp\left(\tfrac{-(mt+x_R-x_r)^2}{2s^2t^2}\right)-\exp\left(\tfrac{-(mt+x_L-x_r)^2}{2s^2t^2}\right)\right] \\ &+\tfrac{1}{4}\left[(x_R-x_l)\left(m^2+s^2+2C\right)+mt\left(m^2+3s^2+2C\right)\right]\operatorname{erf}\left(\tfrac{mt+x_R-x_l}{\sqrt{2}st}\right) \\ &-\tfrac{1}{4}\left[(x_L-x_l)\left(m^2+s^2+2C\right)+mt\left(m^2+3s^2+2C\right)\right]\operatorname{erf}\left(\tfrac{mt+x_L-x_l}{\sqrt{2}st}\right) \\ &-\tfrac{1}{4}\left[(x_R-x_r)\left(m^2+s^2+2C\right)+mt\left(m^2+3s^2+2C\right)\right]\operatorname{erf}\left(\tfrac{mt+x_R-x_r}{\sqrt{2}st}\right) \\ &+\tfrac{1}{4}\left[(x_L-x_r)\left(m^2+s^2+2C\right)+mt\left(m^2+3s^2+2C\right)\right]\operatorname{erf}\left(\tfrac{mt+x_L-x_r}{\sqrt{2}st}\right) \end{aligned} \tag{11}$$

The fluxes that flow into region $x_l$ and $x_r$, where $x_l < x_L$ and $x_r < x_L$, are calculated using similar integrals to those above. To calculate the fraction of mass that remains in the region $x_L - x_R$, we use the result from Eq. 5 and set $x_l = x_L$ and $x_r = x_R$. The same theory also applies to the momentum and energy fluxes using Eqs. 8 and 11. Fig. 1 shows the structured, uniform rectangular mesh to be used for these simulations. To calculate mass flow into the cell directly northeast of cell C, we multiply the original mass in cell C by the fraction of the flow in the $x$ direction to land between region $x_3$ and $x_4$, and then multiply this by the fraction of the flow in the $y$ direction to land between region $y_3$ and $y_4$. Thus if, $m_0$ is the total mass in cell C, the mass moving to the North-East cell is

$$M_{NE} = f_{ME} \times f_{MN} \times m_0 \tag{12}$$

The complete flux expressions, including the effects of a body force, can be found in Smith *et al.* [12].

## RESULTS

We have used direction decoupled methods and TDEFM to simulate a 2D imploding shock wave on a rectangular mesh. In the initial condition there is a low pressure cylindrical region, with a radius of $0.5L$, centered on the origin. It is surrounded by a high pressure region (of size $2L \times 2L$) with a sharp discontinuity between the two. A cylindrically symmetric shock wave propagates towards the origin and cylindrical expansion waves propagate into the high pressure region. Advantage was taken of two planes of symmetry to calculate the flow in the first quadrant only. The computation was halted before the shock reached the origin and before the expansion wave reached the edge of the computational domain. The gas obeys an ideal gas equation of state and the ratio of specific heats was $\gamma = 5/3$.

Figs. 2 show density contours calculated with TDEFM and with a direction decoupled method (with interface fluxes calculated with an approximate Riemann solver [11]). The contours are generally quarter circles, as required but the direction decoupled method shows asymmetric behavior. The amount of asymmetry depends on the number of cells used but, regardless of the cell density, TDEFM shows more symmetric results. Asymmetry can also be decreased by implementing 2nd order in time or space methods. However, implementation of increased order in time simulations show that TDEFM remains superior.

Fig. 3 shows the density and temperature along the $x$-axis where the results from different methods are in general agreement as the shock and expansion waves are virtually parallel to the cell interfaces in this region of the flow. As was apparent in Fig. 2 the temperatures can vary significantly at similar distances from the origin. Fig. 4 shows the local variance of temperature in all cells as a function of distance from the origin; that is, the temperatures for all cells with centroid in the range $r$ to $r+dr$ from the origin have been compared. The variance is significantly greater for the direction decoupled methods. With a finer mesh the variance is reduced in all cases, but is always larger for the direction decoupled methods, than for TDEFM.

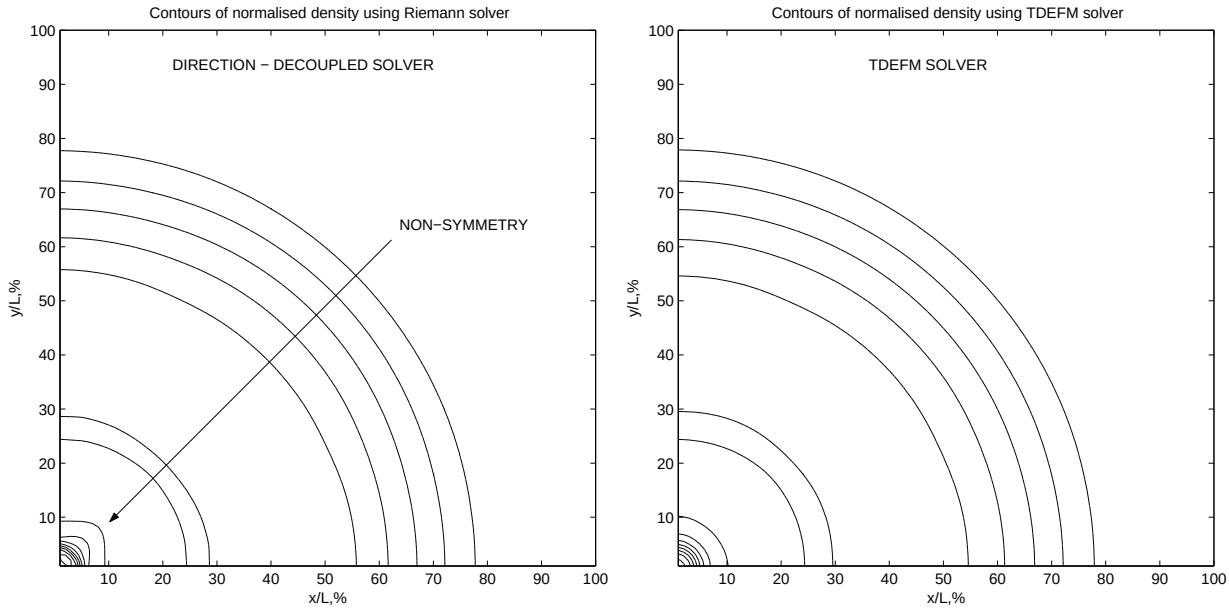


**FIGURE 2.** Contours of normalized density, for direction decoupled Riemann solver (Left) and True Direction Equilibrium Flux Method. (Right) $T_H/T_L = 1$, $\rho_H/\rho_L = 10$. Simulation run for 100 equal time steps until $at/L = 0.296$. $a = \sqrt{\gamma RT_L}$. Each contour represents an increase/decrease of 0.25.

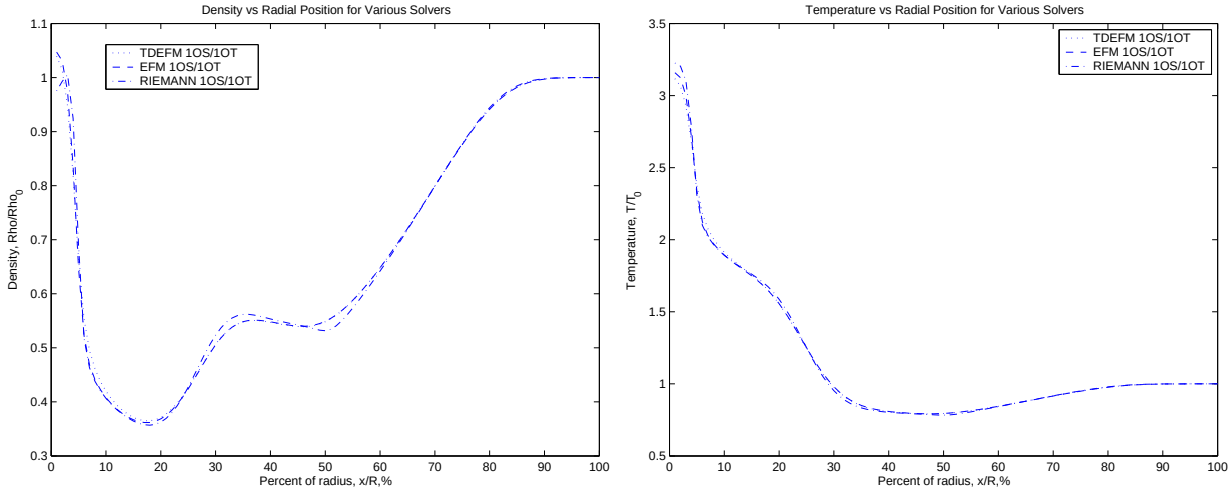


**FIGURE 3.** (Left) Normalized density versus radial position along the x axis. (Right) Normalized temperature versus radial position along the x axis. 1OS = 1st order in space, 1OT = 1st order in time. $T_H/T_L = 1$, $\rho_H/\rho_L = 10$. Simulation run for 100 equal time steps until $at/L = 0.296$; $a = \sqrt{\gamma RT_L}$. Reflection at the origin has not yet occurred. Values are normalized by the initial values in the low pressure region.

## CONCLUSION

TDEFM fluxes are derived from the movement of molecules in all directions; they do not flow only across interfaces between cells. Except for the assumed zero density gradients within cells, 'first-order' TDEFM is equivalent to DSMC applied on a given grid, with a given time step, an infinite number of particles and an infinite collision rate (decoupled from the movement of the particles). To restrict the dissipation associated with molecular free flight, the time-step has been restricted so that fluxes are exchanged between contiguous cells, including diagonally adjacent cells.

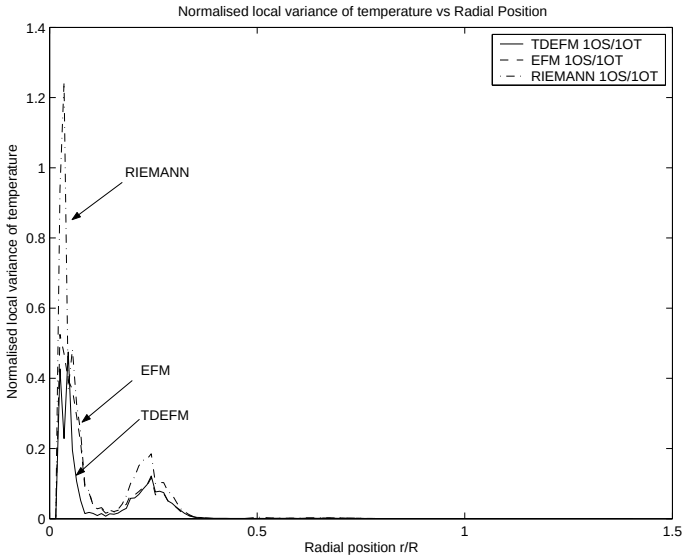


**FIGURE 4.** Normalized variance in local temperature versus radial position for all cells in the flow.

We tested the method in two dimensions by simulating an imploding shock for which the flow structures are not aligned with the grid. We have shown that for this flow the method of direction decoupling, as applied in conventional continuum solvers, leads to asymmetrical results. We have shown that on a structured, uniform rectangular mesh TDEFM can capture un-aligned flows with greater accuracy than the direction decoupled methods. That is, the TDEFM results show a greater degree of cylindrical symmetry than do the results found with direction decoupled methods.

## REFERENCES


1. G. Cook, 'High Accuracy Capture of Curved Shock Fronts Using the Method of Space-Time Conservation Element and Solution Element', 37th American Institute of Aeronautics and Astronautics Aerospace Sciences Meeting and Exhibit, 1998.
2. Pullin, D.I., 'Direct Simulation Methods for Compressible Ideal Gas Flow',*J. Comput. Phys.* **34**: 231-244, 1980.
3. M. N. Macrossan, 'The equilibrium flux method for the calculation of flows with non-equilibrium chemical reactions', *J. Comput. Phys.* **80**: 204-231, 1989.
4. Lengrand, J.C., Raffin, M. and Allegre, J., 'Monte Carlo Simulation Method Applied to Jet Wall Interactions under Continuum Flow Conditions', in Rarefied Gas Dynamics, edited by Fisher, Progress in Astronautics and Aeronautics, **74**, AIAA, New York, 994-1006, 1981.
5. C. L. Merkle, H. W. Behrens and R. D. Hughes, 'Applications of the Monte-Carlo Simulation Procedure in the Near Continuum Regime', *Rarefied Gas Dynamics 12*, edited by Fisher, Progress in Astronautics and Aeronautics, **74**, AIAA, New York, 256–268, 1981.
6. M. N. Macrossan, M. V. Metchnik and P. A. Pinto, 'Hypersonic flow over a wedge with a particle flux method', *Rarefied Gas Dynamics 24*, edited by Capetilli, AIP Conference Proceedings **762**, American Institute of Physics, New York, 650-656, 2005. http://eprint.uq.edu.au/archive/00001819/
7. M. N. Macrossan and R. J. Stalker, 'Afterbody flow of a dissociating gas down-stream of a blunt nose', AIAA paper 87-0407, 1987.
8. M. N. Macrossan, 'Hypervelocity flow of dissociating nitrogen downstream of a blunt nose', *J. Fluid Mech.* **207**: 167-202, 1990.
9. M. N. Macrossan and D. I. Pullin, 'A Computational Investigation of Inviscid Hypervelocity Flow of a Dissociating Gas Past a Cone at Incidence', *J. Fluid Mech.* **266**: 69-92, 1994.
10. E. R. Mallett, D. I. Pullin and M. N. Macrossan,'Numerical study of hpersonic leeward flow over a blunt nosed delta wing',*AIAA J.* **33**: 1626-1633, 1995.
11. P. A. Jacobs, 'MBCNS: A computer program for the simulation of transient compressible flows, 1998 Update', Department of Mechanical Engineering Report 7/98, The University of Queensland, June 1998.
12. M. R. Smith, M. N. Macrossan, M. V. Metchnik and P. A. Pinto, 'True Direction Equilibrium Flux Method Applications on Rectangular 2D Meshes', Department of Mechanical Engineering Report 6/2006, The University of Queensland, March 2006. http://eprint.uq.edu.au/archive/00004058/